



ELSEVIER

Journal of Physics and Chemistry of Solids 61 (2000) 1633–1638

JOURNAL OF  
PHYSICS AND CHEMISTRY  
OF SOLIDS

www.elsevier.nl/locate/jpcs

# Thermally stimulated depolarization and infrared studies in single-crystal dolomite ( $\text{CaMg}(\text{CO}_3)_2$ )

A.N. Papathanassiou\*, J. Grammatikakis

*Section of Solid State Physics, Department of Physics, University of Athens, Panepistimiopolis, 157 84 Athens, Greece*

Received 17 September 1999; accepted 28 January 2000

## Abstract

The thermally stimulated depolarization current technique is employed so as to study the dipole relaxation in dolomite. We traced two dominant low-temperature dispersions; one located at 140 K and another at 188 K. The first is characterized by the distribution in the relaxation time and the latter one has single-valued relaxation parameters. Standard characterization techniques and annealing treatments on dolomite samples with different micro-structural features showed that the dipoles contributing to the 140 K peak are matrix defects, rather than hydrophilic sites in the pore network. The infrared spectroscopy established the absence of water molecules and the presence of hydroxyls, which probably constitute one type of defect dipoles. © 2000 Elsevier Science Ltd. All rights reserved.

*Keywords:* Ionic thermocurrent; Infrared spectroscopy; D. Dielectric properties; Polycrystalline materials

## 1. Introduction

Dielectric relaxation experiments have been conducted so as to probe the effect of mixing on the dipole dynamics in mixed ionic crystals [1–5]. The results were interpreted [1] by considering that the formation of a mixed crystal induces a long-range effect, due to the modification of the lattice constant. On the other hand, the immediate environment of the rotating dipole is different from that of the pure components alone (short-range perturbation). Most of the experimental work on the dielectric relaxation in mixed crystals is limited to simple ionic systems, like the alkali halides and the alkaline earth fluorides [1–5]. Recently, we expanded the research to the field of mixed crystals by working on the calcite type materials: calcite ( $\text{CaCO}_3$ ); magnesite ( $\text{MgCO}_3$ ) and their mixed crystal dolomite ( $\text{CaMg}(\text{CO}_3)_2$ ). The calcite family crystals share the rhombohedral crystal structure [6,7]. The structure is roughly approximated by the sodium chloride structure, with Ca or Mg on the cation site and  $\text{CO}_3$  on the anion site [7]. The potential difference is that the participant of the alkaline earth ion is the trioxycarbon group, which is not a center of symmetry and

accommodates covalent bonds between the oxygen and the carbons.

In a series of papers, we employed the thermally stimulated depolarization current (TSDC) technique to identify and characterize the relaxation mechanisms in the crystals of the calcite group [8–11]. Therein, we proved that the theoretical models, which appeared in the literature previously [1], do not apply to the calcite family. The low-temperature dielectric relaxation spectra of the latter are identified by two dominant mechanisms reaching a maximum at about 140 K and around 188 K, respectively. Following the notation mentioned in Refs. [9–11], we label the aforementioned dispersions LT1 and LT2, respectively. The usual interpretation that the LT1 and the LT2 peaks correspond to two different relaxation modes of the same type of defect dipoles [1] may not apply to the calcite group [8]. In a paper published recently [8], we discussed extensively the low-temperature relaxation in the calcite family materials. We concluded that the formation of the LT1 dispersion is most probably related to the presence of hydroxyls or water molecules in the material. However, it is an open question whether the LT1 mechanism is related to bulk dipole relaxation (i.e. due to the rotation of defect dipoles embedded in the matrix) or to surface relaxation of water (moisture) dipoles, which are either strongly or loosely bound to the grain surface. With the aim of clarifying the

\* Corresponding author. Tel.: + 301-722-4444; fax: + 301-7661707.

above-mentioned questions, we worked in two directions: firstly, we studied the single crystals of dolomite, which have definitely different micro-structures on a nanometer scale in comparison to that of polycrystalline samples. Another open question is about the identity of the LT1 dipoles; i.e. whether they are water dipoles or agglomerates with hydroxyl ions. The IR spectroscopy is employed to give a firm answer.

## 2. Theory

The dielectric relaxation of an insulator originates from the rotation of dipoles and the motion of free charge carriers under certain boundary conditions [12]. In general, we assume that the relaxation time  $\tau$ , which governs the relaxation process, is described by the Arrhenius law:

$$\tau(T) = \tau_0 \exp\left(\frac{E}{kT}\right) \quad (1)$$

where  $E$  denotes the activation energy,  $\tau_0$  the pre-exponential factor and  $k$  the Boltzmann's constant. The TSDC method consists of the following steps [13]. The specimen is polarized at the temperature  $T_p$  for a time interval  $t_p \gg \tau(T_p)$  and, subsequently by keeping the external polarizing field on, we freeze to the liquid nitrogen temperature (LNT), where the relaxation time is practically infinite. As a result, on removing the electric field, the dielectric remains polarized. Then, we heat the sample at a constant heating rate  $b$ . At the same time, the depolarization current is recorded via a sensitive electrometer. At the temperature region, where the thermal energy competes with the energy  $E$  needed for the reorientation of the polarized dipoles, we get an asymmetric transient electric signal, which is called "thermogram". The different types of dipoles, or the dispersions of the interfacial and the frozen space charge polarizations, give rise to different TSDC peaks.

The reorientation of non-interacting dipoles stimulates the depolarization current:

$$I(T) = \frac{SII_0}{\tau_0} \exp\left[-\frac{E}{kT} - \frac{1}{b\tau_0} \int_{T_0}^T \exp\left(-\frac{E}{kT}\right) dT\right] \quad (2)$$

where  $II_0$  is the initial polarization of the dielectric,  $S$  the sample's surface area which is in contact with the electrode and  $T_0$  is identical to the LNT. Regarding a defect dipole, which consists of a vacancy associated to an heterovalent impurity, the activation energy  $E$  is identical to the migration enthalpy  $h^m$  of the bound vacancy around the impurity (which is considered to be immobile) [14].

For the initial part of the curve, Eq. (2) is approximated by:

$$I(T) \cong \frac{SII_0}{\tau_0} \exp\left(-\frac{E}{kT}\right) \quad (3)$$

Eq. (3) may lead to the *estimation* of the activation energy  $E$ , when a straight line is fitted to the  $\ln I(T)$  initial rise data.

Assuming that the activation energy is not single valued but has a Gaussian distribution around  $E_0$ , with distribution function [15,16]:

$$f(E) = \frac{1}{\sqrt{2\pi}\sigma} \exp\left[-\frac{(E-E_0)^2}{2\sigma^2}\right] \quad (4)$$

where  $\sigma$  is the broadening parameter and the total depolarization current can be written as:

$$I(T) = \int_{-\infty}^{+\infty} f(E)I(T, E) dE \quad (5)$$

where the term  $I(T, E)$  is the monoenergetic TSDC equation (see Eq. (2)).

The integral of Eq. (2) can be approximated by the following analytical expression:

$$\int_{T_0}^T \exp\left(-\frac{E}{kT}\right) dT = \frac{T \exp(-E/kT)(E/kT + 3.0396)}{(E/kT)^2 + 5.0364(E/kT) + 4.1916} \Big|_{T_0}^T \quad (6)$$

while the integration of Eq. (6) can be performed from 0 to  $3E_0$  [16].

In order to analyze distributed TSDC signals, the distribution in the relaxation time can be prescribed and a modified TSDC equation can be constructed, in the way mentioned above. To overcome the difficulty in selecting an arbitrary distribution function, it is more preferable to derive the distribution from the experimental data, if possible [12]. The initial rise edge of a distributed peak merely gives an estimate of the activation energy for the fast relaxation mechanisms. In order to evaluate the activation energy, except for the fast (low-temperature) mechanisms, and for the entire temperature region, we must conduct successive partial discharges of the mechanisms. An approximate value for the activation energy corresponds to each initial rise signal, given by Eq. (3). Subsequently, a set of initial rise curves provides actually the temperature distribution of the activation energy. The accuracy of this method is better for the temperature region close to the maximum of the initial peak [17]. The experimental scheme is known as partial heating [18].

## 3. Experimental details

The experiments were conducted in a cryostat operating from the LNT up to 400 K. An Alcatel molecular vacuum pump maintains a vacuum of about  $10^{-5}$  mbar. The crystals were placed between the platinum electrodes and were polarized by using a Keithley 246 DC power supply. The temperature is measured by means of a gold–chromel thermocouple, which is connected to an Air-Products temperature controller. The temperature rise was monitored by the controller, which maintains the required constant heating rate. The depolarization current is recorded through a Cary 401 electrometer. The output signals from the controller and the electrometer are digitized via a Keithley DAS

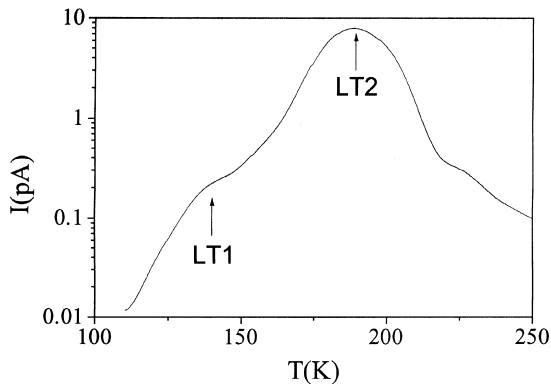


Fig. 1. The low-temperature spectrum of single-crystal dolomite. The polarization temperature was  $T_p = 190$  K and the polarization time  $t_p = 2$  min. It is obvious that the end tail of the signal suffers from strong high-temperature contribution. Different polarization modes that minimize the undesirable overlap are given in detail in the text.

8PGA card, which is installed into a computer. The additional IR spectroscopic investigations were performed at room temperature on a Jasco IR-700 double beam infrared spectrophotometer.

We studied natural single crystals of dolomite from Oberdorf, Styria (Austria). For the same crystal, structural and spectroscopic investigations have been performed previously [19,20]. The specimens were clear and prepared along the cleavage planes. The chemical analysis is cited in Ref. [21] (in wt%): CaO, 30.1; MgO, 20.4; FeO, 1.8; and MnO, 0.5. Additional analyses in the Institute of Geological and Mining Research (IGME, Greece), gave the following results (in wt%): Si, 0.9; Al, 0.02; Sr, 0.02; K, <0.01; Na, 0.03, humidity 0.38.

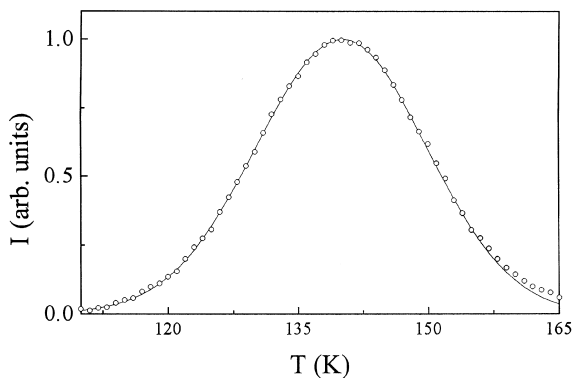


Fig. 2. The LT1 normalized signal (open circles) of the single-crystal dolomite. The peak was cleaned by polarizing at  $T_p = 140$  K for  $t_p = 1$  min, in combination with partial discharge from the LNT to about 120 K. The solid line represents the theoretical curve that best matches the data points. The relaxation parameters are:  $E_0 = 0.360$  eV,  $\sigma = 0.022$  eV and  $\tau_0 = 1.6770 \times 10^{-11}$  s.

#### 4. Results and discussion

Naturally developed crystals are rich in impurities. As a result, the amount of free charges available is considerably large and they participate in the space charge relaxation processes. The presence of a strong space charge mechanism does not only mask a wide temperature region of the TSDC thermogram, but may also affect the polarization state of the dipolar mechanisms. In the polarization stage of a usual TSDC experiment, the formation of space charge reduces the total electric field intensity, which is exerted on the dipoles, in relation to the external electric field that is applied to the specimen. As a result, dipolar peaks may be so weak so that they are not detected during the TSDC scan. Moreover, the spatial distribution of free charges may influence the reorientation of dipoles during the heating (depolarization) stage of the TSDC procedure. In conclusion, it is necessary to minimize the space charge contribution to the TSDC spectrum. In some recently published papers [8,10], we definitely altered the space charge formation by appropriate selection of the polarization temperature.

The low-temperature thermal depolarization spectrum of single-crystal dolomite accommodates two distinct peaks (Fig. 1). The first one reaches a maximum at 140 K and is labeled LT1. The other one (labeled LT2) is drastically masked by the higher broad relaxation mechanisms. The reduction of the spurious contributions was attained by employing various polarization modes and revealed its maximum around 188 K. Details concerning the sampling methods are given in the following discussion.

##### 4.1. Characterization and evaluation of the relaxation parameters of the LT1 band

In Fig. 2, we depict the thermograms obtained by polarizing at temperatures low enough to isolate the LT1 mechanism, which is located at 140 K. For polarization temperatures below 140 K, the peak amplitude decreases with the maximum shifting towards lower temperatures, and the mechanism is characterized by distribution in the relaxation time. A knee appearing in the initial part of the depolarization current (around 115 K) originates from a weak satellite peak.

By employing platinum electrodes, we performed four successive measurements under exactly the same polarization conditions:  $T_p = 140$  K,  $E_p = 30$  kV/mm,  $t_p = 2$  min. A set of four scans was conducted by using bronze electrodes, and four for Teflon (insulating) electrodes. The procedure was repeated for a sample with silver-pasted surfaces. In all cases, the peak was reproducible and insensitive to the electrode material.

We polarized the mechanism completely ( $T_p = 140$  K) with a field intensity  $E_p = 30$  kV/cm and we performed the experiment for various polarization time intervals:  $t_p = 1, 2, 4$  and 8 min. We observed that the polarization for 1 min is adequate to polarize the mechanism to saturation.

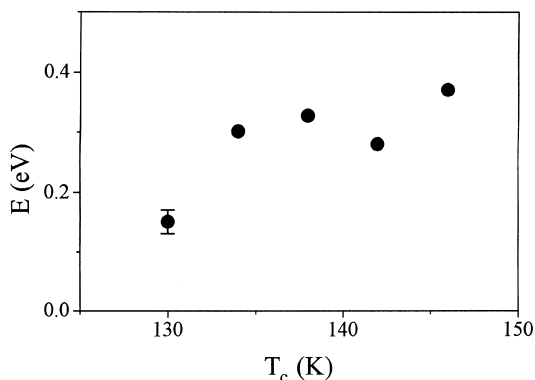


Fig. 3. Temperature distribution of the activation energy values for the LT1 mechanism of single-crystal dolomite, obtained by the partial heating experiments.

By keeping the polarization temperature and the polarization time constant ( $T_p = 140$  K and  $t_p = 2$  min), we varied the electric field intensity  $E_p$  and concluded that the peak amplitude increases linearly with  $E_p$ . The reproducibility, the non-dependence on the electrode material and the saturation in small polarization time interval firmly establish the dipolar nature of the LT1 band. At this point, we note that the linear dependence of the signal amplitude on the polarization field intensity cannot be the only firm criterion for dielectric characterization.

A specimen of single-crystal dolomite was annealed at 400°C for a time interval of 30 min, and was then quenched to the room temperature. A successive TSDC experiment showed that the LT1 is not practically affected by thermal perturbation. It seems that the LT1 dipole population is quite stable and the thermal annealing does not lead to the formation of new dipole agglomerates.

In Fig. 2, we depict the LT1 band, obtained after careful

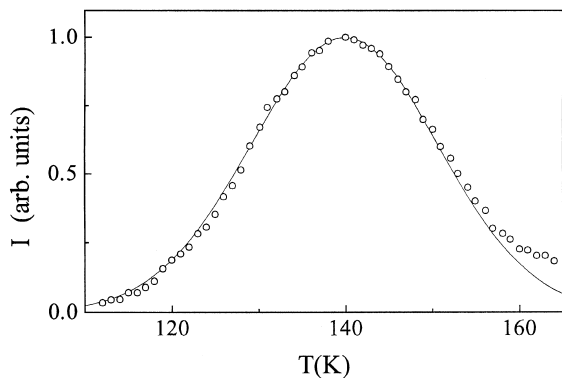


Fig. 4. The LT1 band (circles) recorded in a sample of polycrystalline dolomite, by polarizing at 140 K for the time interval  $t_p = 1$  min. The solid line is the theoretical curve that best matches the experimental points. The relaxation parameters are  $E_0 = 0.351$  eV,  $\sigma = 0.024$  eV and  $\tau_0 = 3.6733 \times 10^{-11}$  s.

cleaning.; i.e. polarizing the maximum of the LT1 peak for  $t_p = 1$  min, and discharging up to 120 K in the depolarization (heating) stage. A successive heating procedure yielded the isolated LT1 band (Fig. 2). Assuming that the activation energy values obey the normal distribution around a central value  $E_0$ , we performed a nonlinear least squares fit of Eq. (5) to the experimental data points. The result was visually inspected so as to have a good match of the theoretical curve to the initial part of the signal. The best relaxation parameters are  $E_0 = 0.360$  eV,  $\sigma = 0.022$  eV and  $\tau_0 = 1.6770 \times 10^{-11}$  s.

In order to overcome the problem of the arbitrary selection of a distribution function, we estimated the activation energy values experimentally by employing the partial heating scheme [21], whereas no assumption about the distribution function is required. It consists of partial discharges of a polarized mechanism at constant temperature step. The discharge is interrupted at the temperature  $T_c$ , as soon as the initial part of the depolarization current appears. Eq. (3), when fitted to the initial rise data, provides an approximate value of the activation energy. The temperature distribution of the activation energy values is displayed in Fig. 3. The first (low-temperature) data point is unreliable, due to the presence of the low-temperature satellite dispersion mentioned above. We conclude that the activation energy values range from 0.28 to 0.37 eV. Although the energy span is about four  $\sigma$ , the energy values, which were estimated experimentally, are compatible with the energy spectrum obtained from the whole curve fitting. It is probable that  $\sigma$  is actually suppressed as a consequence of the partial discharge required in order to eliminate the low-temperature satellite dispersion.

#### 4.2. On the origin of the LT1 dispersion: effect of microstructure modification and identification of hydroxyl through IR spectroscopy

The LT1 band appears in the thermograms of polycrystalline dolomite, as well [10]. The activation energy values obtained by the partial heating scheme range from 0.24 to 0.40 eV. Additional experiments on polycrystalline dolomite were performed in the present work, so as to obtain a well-cleaned curve of the LT1 band (Fig. 4). The relaxation parameters of the theoretical curve that best matches the data points, are:  $E_0 = 0.351$  eV,  $\sigma = 0.024$  eV and  $\tau_0 = 3.6733 \times 10^{-11}$  s.  $E_0$  is about 3% lower than that evaluated for the single crystal. The migration enthalpies corresponding to the rotation of the LT1 dipoles are practically identical. The larger value of the  $\sigma$  parameter obtained for the polycrystalline specimen stems from the perturbation caused by the internal boundary conditions (i.e. the grain boundaries). From the area under the TSDC signal, we found that the LT1 dipole concentration is the same for both the polycrystalline and the single-crystal specimen and thus the divergence between the broadening parameters

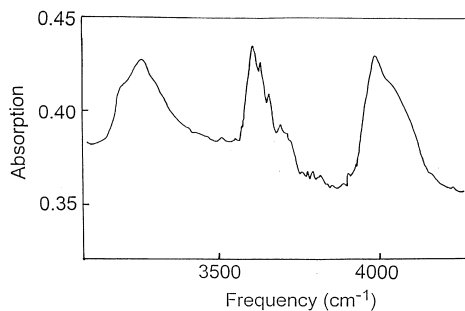


Fig. 5. Absorption IR spectrum of single-crystal dolomite.

can hardly be attributed to electrostatic interactions resulting from the dipole concentration.

We proposed recently [8] that the LT1 mechanism originates from the rotation of water molecules or defect dipoles with hydroxyl as the major participant. The incorporation is favored by the magnesium sublattice [22]. There are three possibilities for the location of the LT1 dipoles: (a) they are accommodated in the pores of the polycrystalline specimen; (b) they are (strongly) bound to the grain boundaries, or (c) they are inserted into the matrix material. If hypotheses (a) and (b) were true, the LT1 should be absent in the spectrum of the single crystal. If we consider the pore space or the grains' surface as hydrophilic sites, the charge release of the LT1 mechanism would be porosity dependent, but the latter does not occur. An additional reason for rejecting the first assumption is that the LT1 location and charge release are not influenced by thermal annealing [8]. We conclude that assertion (c) is compatible with the experimental results. The dipoles of the LT1 mechanism are actually lattice defects and are strongly bound to the magnesium sublattice.

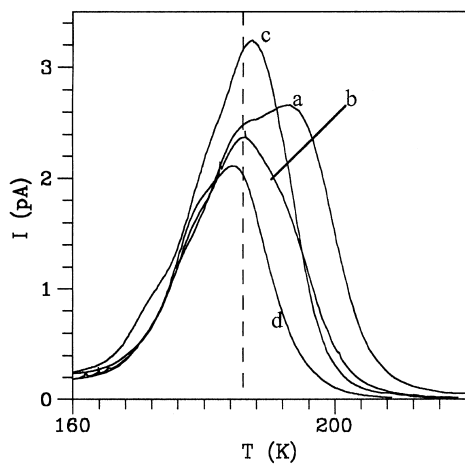


Fig. 6. Tracing the maximum of the LT2 band by varying the polarization temperature  $T_p$ . We employed platinum electrodes. The polarization conditions were:  $E_p = 30$  kV/cm,  $t_p = 1-2$  s and (a)  $T_p = 185$  K, (b)  $T_p = 180$  K, (c)  $T_p = 177$  K, and (d)  $T_p = 175$  K.

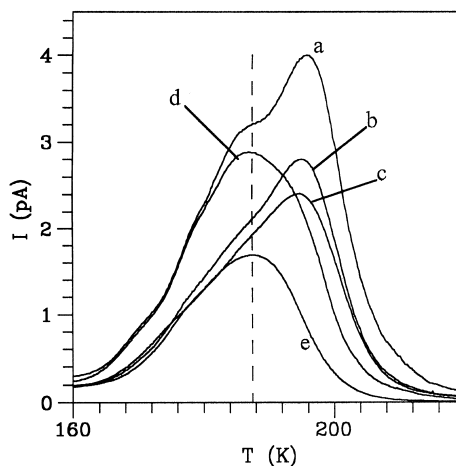


Fig. 7. Minimization of the high-temperature spurious contribution, by reducing the polarization time  $t_p$ : (a) 5 min; (b) 2 min; (c) 1 min; (d) 5 s; (e) 1–2 s. The polarization conditions were:  $E_p = 30$  kV/cm,  $T_p = 180$  K.

Another question is whether water molecules or hydroxyl complexes produce the LT1 dispersion. We performed infrared experiments. In Fig. 5, the absorption vs the frequency is depicted. We emphasize on two peaks, which reach their maxima at  $3300$  and  $3600$   $\text{cm}^{-1}$ . The peaks are located within the frequency region  $3100-3600$   $\text{cm}^{-1}$ , where both the stretching modes of water and hydroxyl should appear [23]. However, the region around  $1600$   $\text{cm}^{-1}$ , where the bending mode of the water appears, is free of any peak. Subsequently, the peaks at  $3300$  and  $3600$   $\text{cm}^{-1}$  are induced by hydroxyl ions [23]. As a result, the LT1 dipoles are rather defect dipoles with hydroxyl in their structure, than freely rotating water molecules.

#### 4.3. Detection of the LT2 dispersion

A strong band, which is labeled LT2, is located around  $188$  K, but it is masked by intense relaxation mechanisms, which activate at higher temperatures. The dispersion is also present in the thermograms of the calcite compounds [8]. We applied an electric field of intensity  $E_p = 30$  kV/cm, for a very short time interval  $t_p = 1-2$  s and performed a series of TSDC experiments for different polarization temperatures  $T_p = 185, 180, 177$  and  $175$  K. In Fig. 6, we see that the reduction of the polarization temperature prohibits the spurious high-temperature contribution and enables the detection of a maximum around  $188$  K. We see that the latter maximum depends slightly on the polarization temperature. We assert that the activation energy is characterized by a very narrow distribution around a central value.

In Fig. 7, we depict a series of thermograms obtained by polarizing for different time intervals:  $t_p = 5$  min, 2 min, 1 min, 5 s and 1–2 s. The polarization temperature was selected so as to minimize the high-temperature spurious

contribution. We observe that the reduction of the polarization time  $t_p$  yields the minimization of the high-temperature contributions. At this point, we note that the effective polarization time in TSDC experiments is larger than  $t_p$ , because of the time required to cool the sample.

It is hard to determine the relaxation parameters by fitting a modified TSDC curve to the whole experimental data points, due to the undesirable neighboring contributions. A crude estimate of the activation energy was obtained by the partial heating scheme:  $E = (0.58 \pm 0.06 \text{ eV})$ . The dispersion in the activation energy values may not be interpreted within the frame of the distribution in  $E$ ; in the preceding paragraph, we showed experimentally that the mechanism is rather non-distributed. Thus, the energy-spread is attributed to the fact that the equation (Eq. (3)) used for analyzing the partial heating signals is actually approximate.

## 5. Conclusion

The 140 K dipole dispersion (LT1 band) of dolomite is related to the rotation of defect dipoles with either hydroxyl as major participant or water molecules. We investigated whether the dipole centers are hydrophilic sites on the surface of polycrystalline aggregates or they are bulk (matrix) defects, which are accommodated by the magnesium carbonate sublattice. Standard characterization techniques and annealing treatments on dolomite samples with different micro-structural features, showed that the dipoles related to the LT1 peak are matrix defects. The full curve fitting yielded the energy spectrum and the pre-exponential factor. Infrared spectroscopic studies proved that the LT1 dipoles are rather defect dipoles consisting of hydroxyl ions than freely rotating water dipoles. This is in agreement with the previous assertion that the defects are matrix ones. Another dispersion (LT2 band) is located around 188 K and manifests as a typical relaxation mechanism of the calcite sublattice.

## Acknowledgements

The authors are grateful to Associate Professor C.A. Londos and Mr E. Fytros for providing the facilities of the IR spectrometer.

## References

- [1] R. Robert, R. Barboza, G.F.L. Ferreira, M. Ferreria de Souza, *Phys. Status Solidi (b)* 59 (1973) 335.

- [2] S.C. Zílio, M. de Souza, *Phys. Status Solidi (b)* 80 (1977) 597.  
 [3] T. Ohgaku, N. Takeuchi, *Phys. Status Solidi (a)* 42 (1977) K83.  
 [4] A. Clark, R. Perez, R. Aceves, A. Hernandez, O.J. Rubio, *Cryst. Latt. Def. Amorph. Mater.* 14 (1987) 91.  
 [5] M.V.S. Sarma, S.V. Suryanarayana, *J. Mater. Sci.: Mater. Electron.* 1 (1990) 182.  
 [6] W.A. Deer, R.A. Howie, J. Zussman, *An Introduction to the Rock Forming Minerals*, Longman, Essex, 1966.  
 [7] R.J. Reeder, *Crystal chemistry of rhombohedral carbonates*, in: R.J. Reeder (Ed.), *Reviews on Mineralogy, Carbonates: Mineralogy and Chemistry*, vol. 11, Mineralogical Society of America, Washington, DC, 1983, p. 1.  
 [8] A.N. Papathanassiou, J. Grammatikakis, *Phys. Rev. B* 56 (1997) 8590.  
 [9] A.N. Papathanassiou, J. Grammatikakis, V. Katsika, A.B. Vassilikou-Dova, *Radiat. Effects Defects Solids* 134 (1995) 247.  
 [10] A.N. Papathanassiou, J. Grammatikakis, *Phys. Rev. B* 53 (1996) 16252.  
 [11] N.G. Bogris, J. Grammatikakis, A.N. Papathanassiou, in: O. Kanert, J.-M. Spaeth (Eds.), *Proceedings of the XII International Conference on Defects in Insulating Materials ICDIM92 (Germany, 1992)*, World Scientific Publishing, Singapore, 1993, p. 804.  
 [12] J. Vanderschueren, J. Gasiot, in: P. Braunlich (Ed.), *Field Induced Thermally Stimulated Currents in Thermally Stimulated Relaxation in Solids*, Springer, Berlin, 1979.  
 [13] C. Bucci, R. Fieschi, *Phys. Rev. Lett.* 12 (1964) 16.  
 [14] P.A. Varotsos, K.D. Alexopoulos, in: S. Amelinckx, R. Gevers, J. Nihoul (Eds.), *Thermodynamics of Point Defects and Their Relation with Bulk Properties*, North-Holland, Amsterdam, 1985.  
 [15] J.P. Calame, J.J. Fontanella, M.C. Wintersgill, C. Andeen, *J. Appl. Phys.* 58 (1985) 2811.  
 [16] E. Laredo, M. Puma, N. Suarez, D.R. Figueroa, *Phys. Rev. B* 23 (1981) 3009.  
 [17] A.N. Papathanassiou, J. Grammatikakis, N. Bogris, *Phys. Rev. B* 48 (1993) 17 715.  
 [18] R. Creswell, M. Perlman, *J. Appl. Phys.* 41 (1970) 2365.  
 [19] F. Prissok, G. Lehmann, *Phys. Chem. Minerals* 13 (1986) 331.  
 [20] H. Effenberger, K. Mereiter, J. Zemmann, *Zeitschrift für Kristallographie* 156 (1981) 233.  
 [21] R. Creswell, M. Perlman, *J. Appl. Phys.* 41 (1970) 2365.  
 [22] F.T. Mackenzie, W.D. Bischoff, F.C. Bishop, M. Loijens, J. Schoonmaker, R. Wollast, *Magnesian calcites: low temperature occurrence, solubility and solid–solution behaviour*, in: R.J. Reeder (Ed.), *Reviews in Mineralogy, Carbonates: Mineralogy and Chemistry*, vol. 11, Mineralogical Society of America, Washington, 1983, p. 97.  
 [23] C.A. Londos, A.M. Vassilikou-Dova, G. Georgiou, L. Fytros, *Phys. Status Solidi (a)* 133 (1992) 473.